Radiation of Millimeter Waves from a Leaky Dielectric Waveguide with a Light-Induced Grating Layer

MASAYUKI MATSUMOTO, MEMBER, IEEE, MAKOTO TSUTSUMI, MEMBER, IEEE, AND NOBUAKI KUMAGAI, FELLOW, IEEE

Abstract—**A theoretical analysis is presented for the radiation characteristics of millimeter waves in a periodic dielectric waveguide having a light-induced grating layer. The waveguide is assumed to be composed of an insulator (sapphire) slab whose one surface is coated with a high-resistivity semiconductor (silicon) film. A boundary-integral-equation formulation is employed to obtain characteristic solutions of the waveguide. Numerical calculations are made at 94 GHz for both TM and TE polarizations. Estimations of the illumination power required to produce the grating are given.**

The waveguide presented in this paper, in conjunction with a high-power semiconductor diode laser array as a light source, may be developed to operate as an electronically beam-steerable leaky-wave antenna at millimeter-wave frequencies.

I. Introduction

PERIODIC DIELECTRIC waveguides have potential usefulness for application to leaky-wave antennas in dielectric-based millimeter-wave integrated circuits because they are lightweight, rigid, and easily fabricated from uniform dielectric waveguides which are the main constituents of the integrated circuits [1]–[3]. In addition, the grating-type leaky-wave antenna has the advantage that the beam direction can be controlled electronically without any mechanical means.

Assuming that the space harmonic of the -1 order is to be radiated, we can express the main beam direction which is measured from broadside to endfire of the antenna by

$$\phi = \sin^{-1}\left(\frac{\beta}{k_0} - \frac{2\pi}{k_0 d}\right) \tag{1}$$

where β, k_0, and d are the phase constant of the fundamental space harmonic, the free-space wavenumber, and the period of the grating, respectively. Steering of the main beam direction has so far been carried out with the period fixed by changing principally $k_0 d$ with frequency scanning or by changing β/k_0 using p-i-n-diode-loaded dielectric waveguides [4] or ferrite waveguides [5]. If an electronic means of varying the period is available, we would obtain a leaky-wave antenna having a wide beam-scan range at a fixed frequency.

One possible way to attain variable periodicity is to use a high-resistivity semiconductor as a waveguide medium and to create a nonpermanent grating by periodic light illumination on the waveguide surface [6], [7]. The grating is generated through the property that the complex permittivity of semiconductors can be modulated by introducing an electron–hole plasma in the semiconductors with photoexcitation. So far, this property has been widely examined for the control of millimeter-wave propagation along semiconductor waveguides with application to antennas, high-speed switches, phase shifters, modulators, and filters [6]–[14]. In a previous paper [7], the authors presented an analysis of the radiation characteristics of millimeter waves in a periodically plasma-induced semiconductor waveguide. In the analysis, the waveguide was assumed to be made entirely of a semiconductor material. For that case, the plasma generated near the surface of the waveguide will diffuse into the waveguide, so that a stationary high-density plasma will be hard to obtain.

In the present paper, a study is made for an insulator waveguide coated with a thin semiconductor layer in which the generated plasma is confined [15]. Sapphire and silicon are assumed as the insulator and semiconductor materials, respectively [16].

In the following sections, the characteristic equation giving leaky-wave solutions is derived by employing a boundary-integral-equation formulation [17], [18] under the two-dimensional assumption and is solved numerically for both TM and TE polarizations at 94 GHz. Discussions on the dependence of the radiation characteristics on plasma density and dimensions of the grating are presented. Estimations of the illumination power required for the waveguide to operate as an antenna with a reasonable efficiency are also given. Finally, it is mentioned that an electronically beam-switchable leaky-wave antenna may be fabricated from the waveguide by using a high-power semiconductor diode laser array [19]–[21] as a light source.

Manuscript received March 30, 1987; revised July 21, 1987.

M. Matsumoto and M. Tsutsumi are with the Department of Communication Engineering, Faculty of Engineering, Osaka University, Suita, Osaka 565 Japan.

N. Kumagai was with the Department of Communication Engineering, Osaka University. He is now President of Osaka University.

IEEE Log Number 8716912.

0018-9480/87/1100-1033$01.00 ©1987 IEEE

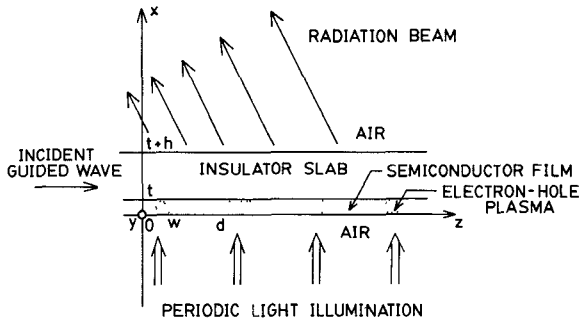

Fig. 1. Side view of a periodic dielectric waveguide having a light-induced grating layer.

II. Waveguide Structure Analyzed in this Paper

Fig. 1 shows a side view of the two-dimensional model of the waveguide analyzed in this paper. The waveguide is made of an insulator slab whose lower surface is covered with a thin, high-resistivity semiconductor film. The layered structure is illuminated periodically from below with optical radiation whose photon energy is larger than the band-gap energy of the semiconductor. The light illumination induces an electron–hole plasma in the film, causing the generation of a complex-permittivity-modulated grating layer. If the period of the grating is chosen properly, the permittivity modulation scatters the incident guided waves continuously in both upward and downward directions. The radiation angle is given by (1).

In this paper, we assume high-purity silicon as the semiconductor material, and sapphire, on which silicon can be deposited epitaxially, as the insulator. Although sapphire is a uniaxial anisotropic material, it can be taken as isotropic with relative permittivity $\epsilon_s = 9.4$ [22] for TM (TE) polarized waves when the optic axis lies in the y direction (in the xz plane) in Fig. 1. The silicon film is desired to be as thin as possible to confine the plasma in a narrow region. However, in order for the illuminated light power to be absorbed efficiently, the thickness of the film cannot be made smaller than the light-penetration depth in silicon. In this paper we shall make numerical calculations for thickness around 30 μm, which is a typical value of penetration depth in silicon of the light emitted from GaAlAs/GaAs diode lasers.

The relative complex permittivity of the semiconductor containing electron–hole pairs of density n is given by

$$\epsilon_p = \epsilon_r - \sum_{\iota = e,h} \frac{\omega_{p\iota}^2}{\omega^2 + \nu_\iota^2}\left(1 + j\frac{\nu_\iota}{\omega}\right)$$

where

$\omega_{p\iota}^2 = ne^2/\epsilon_0 m_\iota$
ω angular frequency of the electromagnetic fields,
e elementary charge,
ϵ_0 permittivity of free space,
ϵ_r relative permittivity of the semiconductor without the plasma,

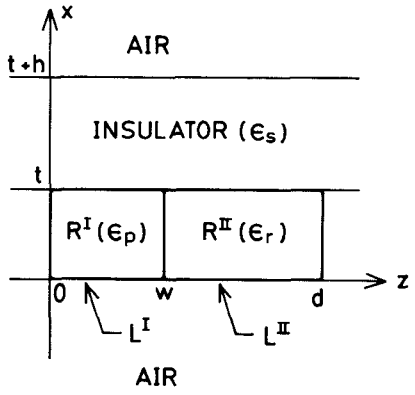

Fig. 2. Unit cell of the periodic waveguide.

m_e (m_h) effective mass of an electron (hole),
ν_e (ν_h) collision angular frequency for electrons (holes).

For silicon, $\epsilon_r = 11.8$, $m_e = 0.259m_0$, $m_h = 0.38m_0$ (m_0 is the electron rest mass), $\nu_e = 4.53\times10^{12}$ s^{-1}, and $\nu_h = 7.71\times10^{12}$ s^{-1} [10]. Since the ν_ι's are larger than ω by about an order at millimeter-wave frequencies around 94 GHz ($\omega = 5.9\times10^{11}$ s^{-1}), silicon behaves as a lossy medium whose conductivity changes almost proportionally to the plasma density.

The photogenerated plasma will diffuse according to its density gradient. The one-dimensional diffusion length of the plasma in semiconductors is given by [23]

$$L_D = \sqrt{\frac{2\mu_e\mu_h}{\mu_e + \mu_h}\frac{k_B T}{e}\tau}$$

where

μ_e (μ_h) mobility of electrons (holes),
k_B Boltzmann constant,
T absolute temperature,
τ lifetime of electron–hole pairs.

For silicon L_D is calculated to be 150 μm for $\tau = 10$ μs at 300 K. In the present analysis, we assume that the thickness of the silicon film is much less than L_D. In this case, the plasma can be considered to distribute itself uniformly in the direction perpendicular to the film in steady state. In the direction parallel to the film, on the other hand, the plasma will diffuse away from the illuminated portions within a range of L_D, resulting in a nonuniform distribution. In the following analysis, however, we use a simple model where the plasma distributes itself uniformly in both directions within regions of rectangular cross section.

III. Mathematical Formulation

A. Integral Equations

In the present analysis, boundary-integral equations are employed as governing equations for the fields inside the grating layer. Fig. 2 shows a unit cell of the periodic waveguide. The plasma-occupied region ($0 < x < t$, $0 < z < w$) and the pure semiconductor region ($0 < x < t$, $w < z < d$) are denoted as R^{I} and R^{II}, respectively. L^{I} and L^{II} are

the contours enclosing R^{I} and R^{II}, respectively. The fields inside each region are governed by the following boundary-integral equations:

$$\frac{1}{2}\phi(r_0^{\mathrm{I}}) = \int_{L^{\mathrm{I}}}\left(\psi^{\mathrm{I}}\frac{\partial\phi}{\partial n} - \phi\frac{\partial\psi^{\mathrm{I}}}{\partial n}\right)dl \qquad \text{for } R^{\mathrm{I}} \quad (2a)$$

$$\frac{1}{2}\phi(r_0^{\mathrm{II}}) = \int_{L^{\mathrm{II}}}\left(\psi^{\mathrm{II}}\frac{\partial\phi}{\partial n} - \phi\frac{\partial\psi^{\mathrm{II}}}{\partial n}\right)dl \qquad \text{for } R^{\mathrm{II}} \quad (2b)$$

where

$$\phi = \begin{cases} H_y & \text{for TM polarization} \\ E_y & \text{for TE polarization.} \end{cases}$$

Here r_0^i is a point on L^i, $\int dl$ denotes the principal value line integral with singularities removed, $\partial/\partial n$ is the outward normal derivative on L^i, and the ψ^i's are the Green's functions in the respective regions ($i = \mathrm{I}, \mathrm{II}$). In this paper we use[1] the Hankel function of the second kind and zeroth order $-(j/4)H_0^{(2)}$ as ψ^i. We discretize the integral equations (2) by expanding the unknown functions ϕ and $\partial\phi/\partial n$ on L^i in terms of subsectional step functions and by locating r_0^i at the midpoint of every boundary segment. The resulting matrix equations have the following form:

$$\boldsymbol{G}^{\mathrm{I}}\boldsymbol{u}^{\mathrm{I}} + \boldsymbol{H}^{\mathrm{I}}\boldsymbol{q}^{\mathrm{I}} = \boldsymbol{0} \quad (3a)$$

$$\boldsymbol{G}^{\mathrm{II}}\boldsymbol{u}^{\mathrm{II}} + \boldsymbol{H}^{\mathrm{II}}\boldsymbol{q}^{\mathrm{II}} = \boldsymbol{0} \quad (3b)$$

where $\boldsymbol{u}^i$ and $\boldsymbol{q}^i$ ($i = \mathrm{I}, \mathrm{II}$) are unknown column vectors whose elements are ϕ and $\partial\phi/\partial n$, respectively, on each segment. $\boldsymbol{G}^i$ and $\boldsymbol{H}^i$ ($i = \mathrm{I}, \mathrm{II}$) are square coefficient matrices whose order is equal to the number of segments into which L^i is divided.

B. Fields in the Uniform Layers

We expand the field ϕ in the uniform layers $t + h < x$, $t < x < t + h$, and $x < 0$ into series of space harmonics as follows:

$$t + h < x \qquad \phi = \sum_m a_m e^{-j\rho_m(x-t-h)}e^{-j\beta_m z} \quad (4a)$$

$$t < x < t + h \qquad \phi = \sum_m (b_m \cos\sigma_m x + c_m \sin\sigma_m x)e^{-j\beta_m z} \quad (4b)$$

$$x < 0 \qquad \phi = \sum_m d_m e^{j\rho_m x}e^{-j\beta_m z} \quad (4c)$$

where

$$\beta_m = \beta_0 + 2m\pi/d$$

$$\rho_m = (k_0^2 - \beta_m^2)^{1/2}$$

$$\sigma_m = (k_0^2\epsilon_s - \beta_m^2)^{1/2}.$$

[1] We can use the Bessel function of the second kind and zeroth order $(1/4)N_0$ as the Green's function as well [17]. In the present analysis, however, since the argument of ψ^{I} possibly has a large negative imaginary part, we had better use $H_0^{(2)}$ in order to carry out numerical calculations stably.

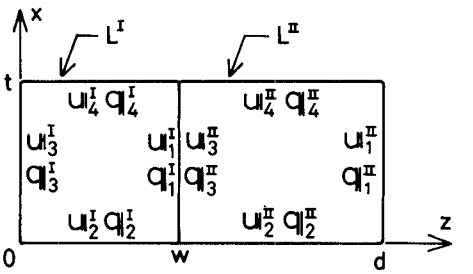

Fig. 3. Unknown vectors on each side of L^{I} and L^{II}.

Here a_m, b_m, c_m, and d_m are amplitudes of the space harmonics, and β_0 is the complex propagation constant of the fundamental space harmonic to be determined.

C. Boundary and Periodicity Conditions

We subdivide the vectors $\boldsymbol{u}^i$ and $\boldsymbol{q}^i$ ($i = \mathrm{I}, \mathrm{II}$) into $\boldsymbol{u}_j^i$'s and $\boldsymbol{q}_j^i$'s ($j = 1$–4), respectively, each of which belongs to each side of L^i (see Fig. 3). The continuity of tangential electromagnetic fields across the boundaries $x = t$ and $x = t + h$ relates $\boldsymbol{u}_4^{\mathrm{I}}, \boldsymbol{u}_4^{\mathrm{II}}$ and $\boldsymbol{q}_4^{\mathrm{I}}, \boldsymbol{q}_4^{\mathrm{II}}$, to each other with the intermediation of the fields described by (4a) and (4b). The resulting equation can be written in the form [17]

$$\begin{pmatrix} \boldsymbol{q}_4^{\mathrm{I}} \\ \boldsymbol{q}_4^{\mathrm{II}} \end{pmatrix} = \begin{pmatrix} \boldsymbol{C}^{\mathrm{I,I}} & \boldsymbol{C}^{\mathrm{I,II}} \\ \boldsymbol{C}^{\mathrm{II,I}} & \boldsymbol{C}^{\mathrm{II,II}} \end{pmatrix}\begin{pmatrix} \boldsymbol{u}_4^{\mathrm{I}} \\ \boldsymbol{u}_4^{\mathrm{II}} \end{pmatrix}. \quad (5)$$

A similar equation holds for the fields at $x = 0$:

$$\begin{pmatrix} \boldsymbol{q}_2^{\mathrm{I}} \\ \boldsymbol{q}_2^{\mathrm{II}} \end{pmatrix} = \begin{pmatrix} \boldsymbol{D}^{\mathrm{I,I}} & \boldsymbol{D}^{\mathrm{I,II}} \\ \boldsymbol{D}^{\mathrm{II,I}} & \boldsymbol{D}^{\mathrm{II,II}} \end{pmatrix}\begin{pmatrix} \boldsymbol{u}_2^{\mathrm{I}} \\ \boldsymbol{u}_2^{\mathrm{II}} \end{pmatrix}. \quad (6)$$

Boundary conditions at $z = w$ and periodicity conditions imposed on the fields at $z = 0$ and $z = d$ are given by

$$\begin{cases} \boldsymbol{u}_1^{\mathrm{I}} = \boldsymbol{u}_3^{\mathrm{II}} & (7a) \\ \nu^{\mathrm{I}}\boldsymbol{q}_1^{\mathrm{I}} = -\nu^{\mathrm{II}}\boldsymbol{q}_3^{\mathrm{II}} & (7b) \end{cases}$$

and

$$\begin{cases} \boldsymbol{u}_1^{\mathrm{II}} = e^{-j\beta_0 d}\boldsymbol{u}_3^{\mathrm{I}} & (8a) \\ \nu^{\mathrm{II}}\boldsymbol{q}_1^{\mathrm{II}} = -\nu^{\mathrm{I}}e^{-j\beta_0 d}\boldsymbol{q}_3^{\mathrm{I}} & (8b) \end{cases}$$

respectively, where

$$\nu^{\mathrm{I}} = \begin{cases} 1/\epsilon_p & (\mathrm{TM}) \\ 1 & (\mathrm{TE}) \end{cases} \quad \text{and} \quad \nu^{\mathrm{II}} = \begin{cases} 1/\epsilon_r & (\mathrm{TM}) \\ 1 & (\mathrm{TE}). \end{cases}$$

D. Characteristic Equation

The discretized integral equations (3) can be written using $\boldsymbol{u}_j^i$ and $\boldsymbol{q}_j^i$ ($i = \mathrm{I}, \mathrm{II}$, $j = 1$–4) as

$$(\boldsymbol{G}_1^i\boldsymbol{G}_2^i\boldsymbol{G}_3^i\boldsymbol{G}_4^i)\begin{pmatrix} \boldsymbol{u}_1^i \\ \boldsymbol{u}_2^i \\ \boldsymbol{u}_3^i \\ \boldsymbol{u}_4^i \end{pmatrix} + (\boldsymbol{H}_1^i\boldsymbol{H}_2^i\boldsymbol{H}_3^i\boldsymbol{H}_4^i)\begin{pmatrix} \boldsymbol{q}_1^i \\ \boldsymbol{q}_2^i \\ \boldsymbol{q}_3^i \\ \boldsymbol{q}_4^i \end{pmatrix} = \boldsymbol{0} \quad (i = \mathrm{I}, \mathrm{II}).$$

Joining the two equations given above ($i = \mathrm{I}$ and II) and eliminating unknowns with use of (5)–(8) yields a homo-

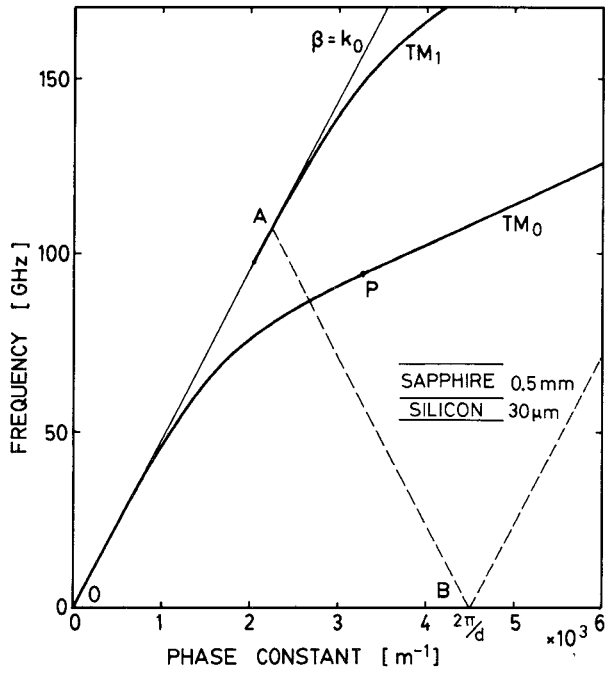

Fig. 4. Dispersion diagram of TM modes for the unperturbed waveguide.

TABLE I
CONVERGENCE OF THE SOLUTION

n (cm^{-3})	N	β (m^{-1})	α (m^{-1})	CPU time (sec)
10^{14}	52	3260.41	3.3616	0.98
	100	3260.55	3.4802	4.73
	200	3260.70	3.4835	27.8
	300	3260.74	3.4866	86.2
10^{16}	52	3366.28	208.12	0.98
	100	3368.19	202.12	5.08
	200	3369.35	199.83	30.4
	300	3369.77	199.22	86.3
10^{18}	52	3619.03	178.90	0.95
	100	3607.76	164.00	5.11
	200	3603.11	158.30	33.1
	300	3601.76	156.69	86.5

TM_0 mode: $h = 0.5$ mm; $t = 30$ μm, $d = 1.4$ mm, and $w = 0.3$ mm.

geneous matrix equation

$$\boldsymbol{A}\boldsymbol{x} = \boldsymbol{0}$$

where

$$\boldsymbol{A} = \begin{pmatrix} \boldsymbol{G}_2^{\mathrm{I}} + \boldsymbol{H}_2^{\mathrm{I}}\boldsymbol{D}^{\mathrm{I,I}} & \boldsymbol{G}_3^{\mathrm{I}} & \boldsymbol{G}_4^{\mathrm{I}} + \boldsymbol{H}_4^{\mathrm{I}}\boldsymbol{C}^{\mathrm{I,I}} & \boldsymbol{H}_3^{\mathrm{I}} & \boldsymbol{H}_2^{\mathrm{I}}\boldsymbol{D}^{\mathrm{I,II}} & \boldsymbol{G}_1^{\mathrm{I}} & \boldsymbol{H}_4^{\mathrm{I}}\boldsymbol{C}^{\mathrm{I,II}} & -\frac{\nu^{\mathrm{II}}}{\nu^{\mathrm{I}}}\boldsymbol{H}_1^{\mathrm{I}} \\ \boldsymbol{H}_2^{\mathrm{II}}\boldsymbol{D}^{\mathrm{II,I}} & e^{-j\beta_0 d}\boldsymbol{G}_1^{\mathrm{II}} & \boldsymbol{H}_4^{\mathrm{II}}\boldsymbol{C}^{\mathrm{II,I}} & -\frac{\nu^{\mathrm{I}}}{\nu^{\mathrm{II}}}e^{-j\beta_0 d}\boldsymbol{H}_1^{\mathrm{II}} & \boldsymbol{G}_2^{\mathrm{II}} + \boldsymbol{H}_2^{\mathrm{II}}\boldsymbol{D}^{\mathrm{II,II}} & \boldsymbol{G}_3^{\mathrm{II}} & \boldsymbol{G}_4^{\mathrm{II}} + \boldsymbol{H}_4^{\mathrm{II}}\boldsymbol{C}^{\mathrm{II,II}} & \boldsymbol{H}_3^{\mathrm{II}} \end{pmatrix}$$

and

$$\boldsymbol{x} = \left[\boldsymbol{u}_2^{\mathrm{I}} \quad \boldsymbol{u}_3^{\mathrm{I}} \quad \boldsymbol{u}_4^{\mathrm{I}} \quad \boldsymbol{q}_3^{\mathrm{I}} \quad \boldsymbol{u}_2^{\mathrm{II}} \quad \boldsymbol{u}_3^{\mathrm{II}} \quad \boldsymbol{u}_4^{\mathrm{II}} \quad \boldsymbol{q}_3^{\mathrm{II}}\right]^T.$$

The characteristic equation is given by

$$\det\left[\boldsymbol{A}(\beta_0)\right] = 0.$$

Solving the equation numerically using Muller's algorithm, for example, we can obtain the complex propagation constant β_0. From the solution for the vector $\boldsymbol{x}$ accompanying β_0, we can calculate the electromagnetic fields along L^i and the space harmonic amplitudes in the uniform layers.

IV. Numerical Results for TM Polarization

Fig. 4 shows a dispersion diagram of TM modes supported by the unperturbed waveguide without periodic light illumination. The thickness of the insulator (sapphire) slab and the semiconductor (silicon) film are 0.5 mm and 30 μm, respectively. The phase constant of the fundamental space harmonic when the periodic permittivity modulation is applied, from which we can predict the radiation angle, does not differ much from the unperturbed phase constant if the plasma density is low or the width of the plasma-occupied region (plasma strip) is small compared with the period. In Fig. 4 we also show the boundaries between the regions where guided waves are purely bounded and where the waves become leaky by dashed lines for $d = 1.4$ mm. The mode operating outside the triangular OAB works as a leaky mode. The calculations which follow are made for the lowest order mode around the point P, where the space harmonic of the -1 order is a backward propagation beam.

Table I shows the convergence of the solution $\beta_0 \triangleq \beta - j\alpha$ for three different values of plasma density. N is the total number of segments into which L^{I} and L^{II} are divided, and is equal to the order of the matrix $\boldsymbol{A}$. It is found that β_0 converges with increasing N. The calculations in this section are carried out with N around 200. In Table I we also show computation times on a NEC SX-1. With regard to the CPU times, it should be noted that the FORTRAN program used in the calculation does not have an architecture optimized for vector processing. The CPU times will be considerably reduced if the capability of the vector machine is fully exploited with a program which has a suitable architecture and is coded suitably for vector processing.

Fig. 5 shows a plot of the phase and attenuation constants of the fundamental space harmonic, β and α, as

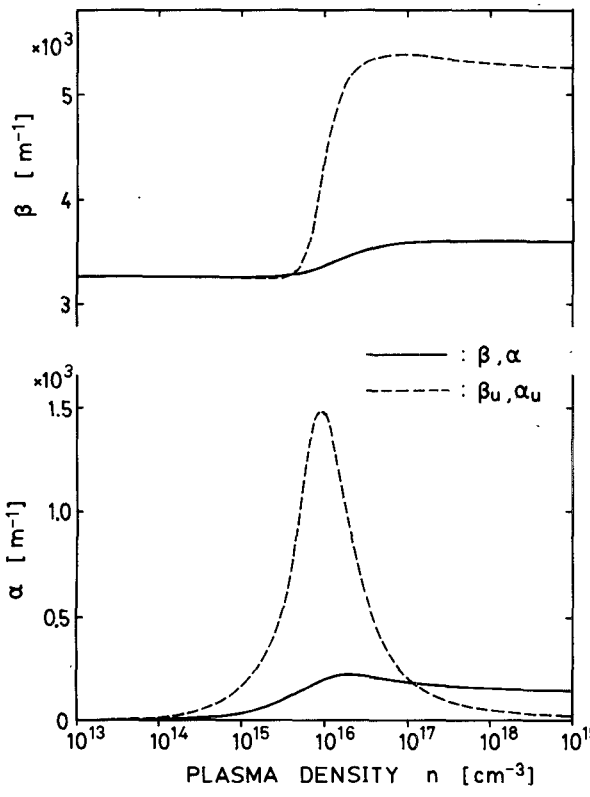

Fig. 5. Phase and attenuation constants of TM_0 mode as functions of plasma density ($h = 0.5$ mm, $t = 30$ μm, $d = 1.4$ mm, and $w = 0.3$ mm).

functions of the plasma density for $d = 1.4$ mm and $w = 0.3$ mm. The value of w is chosen to be twice the diffusion length L_D given in Section II. For comparison, the propagation constants β_u and α_u for a uniformly plasma-induced waveguide ($w = d$) are plotted by dashed lines. When the plasma density is low ($n \lesssim 3\times10^{15}$ cm^{-3}), the plasma strips behave only as a lossy material without scattering much of the guided-wave power out of the waveguide. In this case $\alpha \cong (w/d)\alpha_u$ holds. With higher plasma density ($n \gtrsim 3\times10^{15}$ cm^{-3}), the plasma strips scatter larger power, and the guided wave attenuates due to both dissipation and radiation losses. Increasing the density further, the attenuation constant approaches the leakage constant of the waveguide where the plasma strips are replaced by perfect conductor strips.

In order to specify the magnitude of the plasma density with which the waveguide is taken to operate as an antenna, we must have a knowledge of the ratio of the radiated power to the dissipated power as a function of plasma density. We can calculate the power radiated from a period of the waveguide in the upward and downward directions by

$$P_r^+ \triangleq -\frac{1}{2}\mathrm{Re}\left[\int_0^d E_z^{(-1)}H_y^{(-1)*}\,dz\Big|_{x=t+h}\right]$$

$$= \frac{1}{2\omega\epsilon_0}|a_{-1}|^2\,\mathrm{Re}[\rho_{-1}]\frac{1-e^{-2\alpha d}}{2\alpha}$$

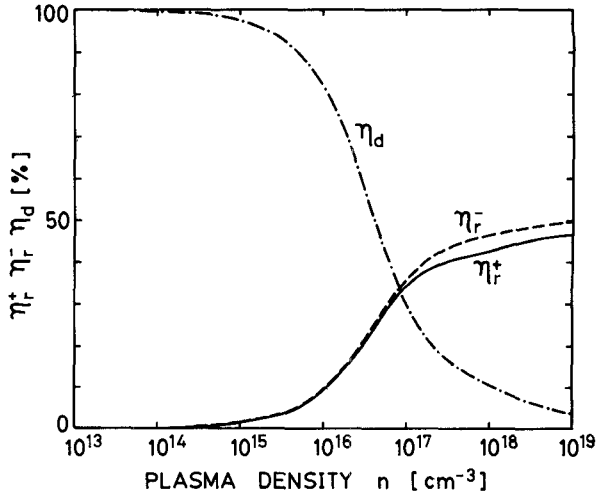

Fig. 6. Percentages of radiation and dissipation powers as functions of plasma density for the TM_0 mode ($h = 0.5$ mm, $t = 30$ μm, $d = 1.4$ mm, and $w = 0.3$ mm).

and

$$P_r^- \triangleq \frac{1}{2}\mathrm{Re}\left[\int_0^d E_z^{(-1)}H_y^{(-1)*}\,dz\Big|_{x=0}\right]$$

$$= \frac{1}{2\omega\epsilon_0}|d_{-1}|^2\,\mathrm{Re}[\rho_{-1}]\frac{1-e^{-2\alpha d}}{2\alpha}$$

respectively, where the superscript (-1) to E_z and H_y means that the values are the space-harmonic components of the -1 order. The power dissipated by the plasma in a period is given by

$$P_d = -\frac{1}{2}\mathrm{Re}\left[\oint_{L^I}(\boldsymbol{E}\times\boldsymbol{H}^*)\cdot\boldsymbol{n}\,dl\right]$$

$$= \frac{1}{2\omega\epsilon_0}\mathrm{Re}\left[-\frac{j}{\epsilon_p}\oint_{L^I}\phi^*\frac{\partial\phi}{\partial n}\,dl\right]$$

where $\boldsymbol{n}$ is an outward normal unit vector on L^I. Fig. 6 shows the ratios of P_r^+, P_r^-, and P_d to the total power:

$$\eta_r^+ = P_r^+/(P_r^+ + P_r^- + P_d) \tag{9a}$$

$$\eta_r^- = P_r^-/(P_r^+ + P_r^- + P_d) \tag{9b}$$

$$\eta_d = P_d/(P_r^+ + P_r^- + P_d) \tag{9c}$$

as functions of plasma density. From the figure, it is found that the percentages of radiation really increase and that of dissipation decreases as the density increases. It can also be seen that radiation occurs almost evenly in the upward and downward directions. For $n = 10^{17}$ cm^{-3}, for example, about 34 percent of the power fed into the leaky mode radiates away effectively into the upper half-space of the waveguide with sufficient length. The quantity η_r^+ can be used as a measure of radiation efficiency.

Fig. 7 shows a plot of the propagation constant and the main beam direction given by (1) as functions of the period. It is found that the main beam direction can be controlled over a wide range by changing the period.

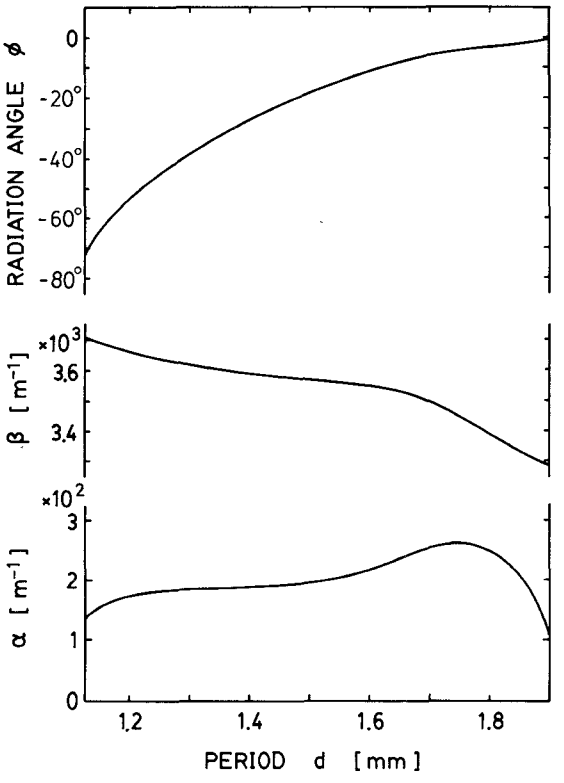

Fig. 7. Radiation angle and the propagation constant of the TM_0 mode as functions of the period ($h = 0.5$ mm, $t = 30$ μm, $w = 0.3$ mm, and $n = 10^{17}$ cm^{-3}).

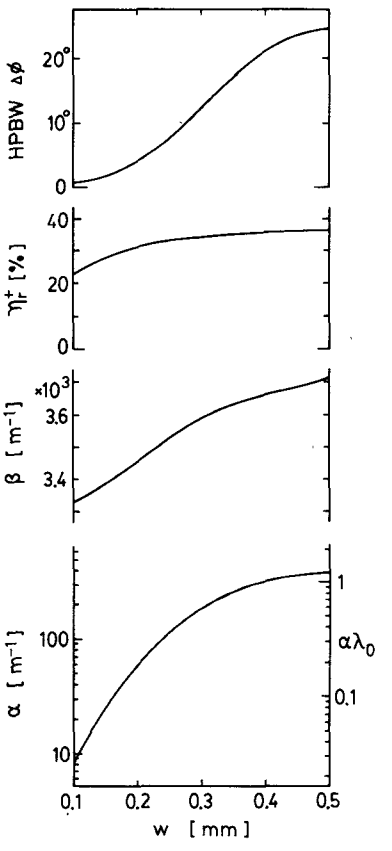

Fig. 8. Dependence of the radiation characteristics on the plasma-strip width for the TM_0 mode ($h = 0.5$ mm, $t = 30$ μm, $d = 1.4$ mm, and $n = 10^{17}$ cm^{-3}).

The half-power beam width can be calculated approximately by

$$\Delta\phi = \sin^{-1}\left(\frac{\beta}{k_0} - \frac{2\pi}{k_0 d} + \frac{\alpha}{k_0}\right) - \sin^{-1}\left(\frac{\beta}{k_0} - \frac{2\pi}{k_0 d} - \frac{\alpha}{k_0}\right).$$

For the plasma-strip width $w = 0.3$ mm, the value which is used in the calculation of Figs. 5–7, and for $d = 1.4$ mm, and $n = 10^{17}$ cm^{-3}, $\Delta\phi$ is 12.3 degrees. This value seems fairly large. Reduction of the beam width can be achieved by narrowing the plasma-strip width. Fig. 8 shows the dependence of the half-power beam width, the radiation efficiency η_r^+, and the propagation constant on the plasma-strip width. With decreasing w, the attenuation constant decreases rapidly, which gives a larger aperture length and consequent reduction of the beam width. The width $\Delta\phi$ is as small as 0.6° for $w = 0.1$ mm. The reduction of the strip width could be realized by introducing impurities, such as gold in silicon [24], which behave as recombination centers into the semiconductor film. The introduction of such impurities will reduce the lifetime and hence the diffusion length.

Finally, Fig. 9 shows the dependence of the radiation efficiency and the propagation constant on the plasma-strip thickness, which is equal to the semiconductor-layer thickness, for a fixed plasma density $n = 10^{17}$ cm^{-3}. The skin depth of the plasma medium for the electromagnetic fields at 94 GHz is 27 μm. From the figure, it can be seen that the efficiency does not increase with increasing thickness beyond the value of the skin depth. Hence, the thickness of

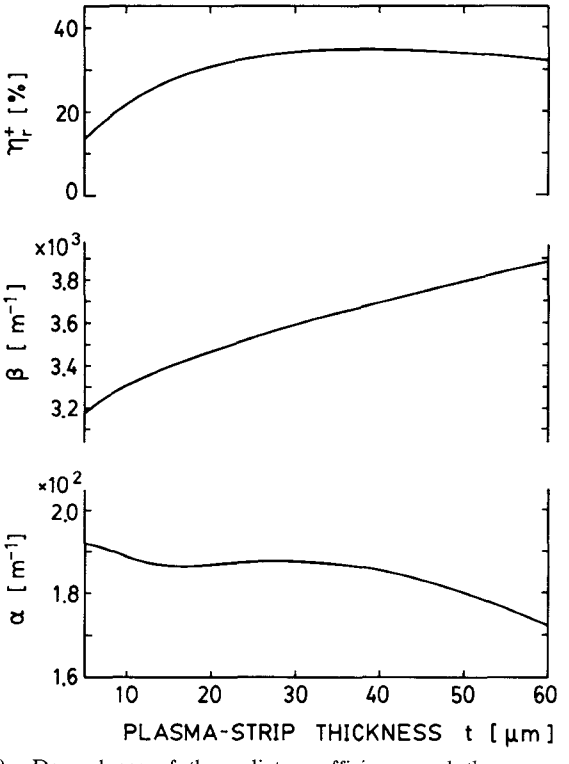

Fig. 9. Dependence of the radiation efficiency and the propagation constant of the TM_0 mode on the plasma-strip thickness ($h = 0.5$ mm, $d = 1.4$ mm, $w = 0.3$ mm, and $n = 10^{17}$ cm^{-3}).

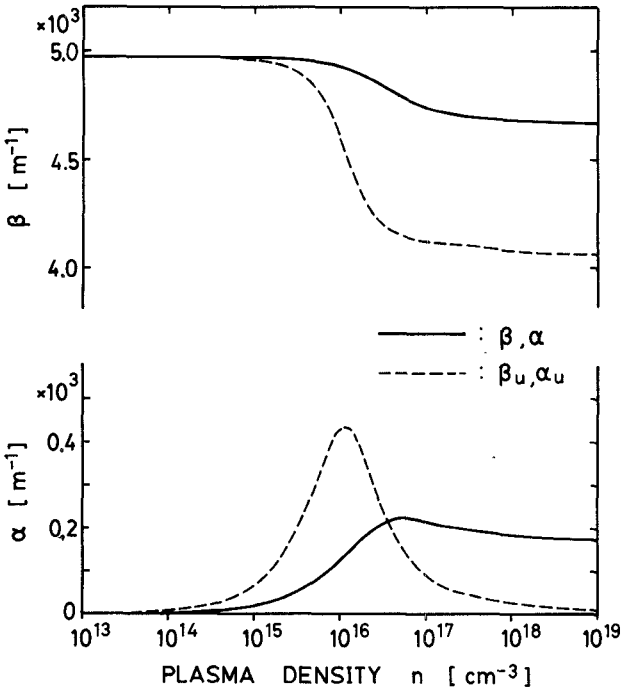

Fig. 10. Phase and attenuation constants of TE_0 mode as functions of plasma density ($h = 0.5$ mm, $t = 30$ μm, $d = 1.1$ mm, $w = 0.3$ mm).

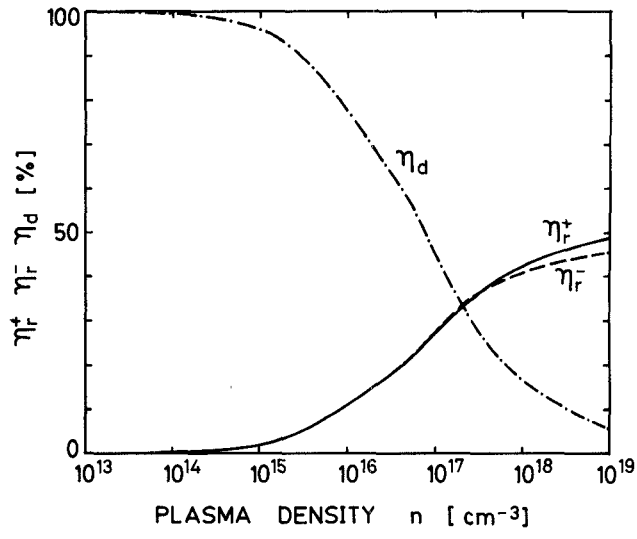

Fig. 11. Percentages of radiation and dissipation powers as functions of plasma density for the TE_0 mode ($h = 0.5$ mm, $t = 30$ μm, $d = 1.1$ mm, and $w = 0.3$ mm).

the semiconductor layer should be chosen approximately equal to the skin depth for a given plasma density in order to save the illumination power to generate the plasma.

V. Numerical Results for TE Polarization

First, convergence of the solution with increasing N was confirmed to be good, as in the case of TM polarization. The following calculations were made with $N \cong 200$.

Fig. 10 shows the propagation constant of the fundamental space harmonic versus plasma density. For this polarization, the phase constant shifts downward as the density increases.

Fig. 11 shows the ratios of the radiated and dissipated powers to the total power as functions of plasma density. The ratios are given by (9), where the powers for the TE case can be calculated by

$$P_r^+ = \frac{1}{2\omega\mu_0}|a_{-1}|^2 \operatorname{Re}[\rho_{-1}]\frac{1-e^{-2\alpha d}}{2\alpha}$$

$$P_r^- = \frac{1}{2\omega\mu_0}|d_{-1}|^2 \operatorname{Re}[\rho_{-1}]\frac{1-e^{-2\alpha d}}{2\alpha}$$

$$P_d = \frac{1}{2\omega\mu_0}\operatorname{Re}\left[j\oint_{L^1}\phi\frac{\partial\phi^*}{\partial n}\,dl\right].$$

The curves shown in Fig. 11 have shapes similar to those in Fig. 6.

Fig. 12 shows the dependence of the half-power beam width given by (10), the radiation efficiency η_r^+, and the propagation constant on the plasma-strip width w. In the

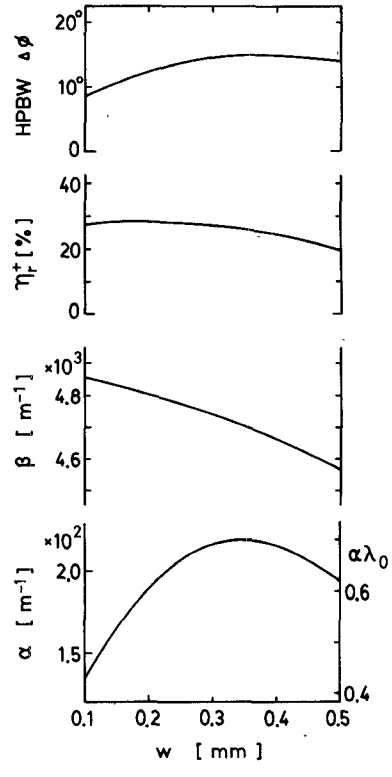

Fig. 12. Dependence of the radiation characteristics on the plasma-strip width for the TE_0 mode ($h = 0.5$ mm, $t = 30$ μm, $d = 1.1$ mm, and $n = 10^{17}$ cm^{-3}).

case of TE polarization, where the electric field lies parallel to the plasma strips, the attenuation constant does not decrease rapidly as the width decreases, in contrast to the TM case [17]. Therefore, the beam width cannot be narrowed sufficiently by decreasing w. To reduce the attenuation constant further when operating with TE polarization, we need to use a more complicated waveguide structure, such as one having a low-permittivity buffer layer between the semiconductor and insulator layers.

VI. Required Illumination Power

In this section, we estimate the optical illumination power required to generate light-induced gratings. Two examples for the operation at 94 GHz with TM polarization are examined:

Example 1:

t (thickness of the silicon film) = 30 μm
d (period of the grating) = 1.4 mm
w (width of a plasma strip) = 0.3 mm
n (plasma density) = 10^{17} cm^{-3}.

Example 2:

w = 0.15 mm
other parameters are the same as in example 1.

Attenuation constants, beam widths, and radiation efficiencies are given in Section IV as

Example 1:

$$\alpha = 188 \text{ m}^{-1}, \quad \Delta\phi = 12.3°, \quad \eta_r^+ = 34.2 \text{ percent}.$$

Example 2:

$$\alpha = 24.6 \text{ m}^{-1}, \quad \Delta\phi = 1.7°, \quad \eta_r^+ = 27.8 \text{ percent}.$$

We determine the antenna length by $L = -\ln 0.05/(2\alpha)$: 5 percent of the fed power is left at the terminal end of the antenna. The numbers of plasma strips, given by L/d, are 6 and 44 for examples 1 and 2, respectively.

The illumination intensity required to generate a steady-state plasma of density n in a semiconductor layer of thickness t is given by

$$I = \frac{\hbar \omega_{\text{opt}} t n}{(1-R)\xi\tau}$$

where

- $\hbar$ Planck's constant divided by 2π,
- ω_{opt} angular frequency of the optical radiation,
- R reflectivity of the light at the semiconductor surface,
- ξ quantum efficiency.

The intensities for the two examples are calculated to be 10.0 W/cm^2 and 40.1 W/cm^2, respectively, using $\lambda_{\text{opt}} = 2\pi/(\sqrt{\epsilon_0\mu_0}\,\omega_{\text{opt}}) = 0.85$ μm, R = 30 percent, $\xi = 1$, and τ = 10 μs for example 1 and τ = 2.5 μs for example 2. The values of the lifetime are those with which the diffusion length L_D is about half of w. The total required illumination power for the two examples assuming that the width of the waveguide in the y direction is 5 mm is as follows:

Example 1: 0.9 W(150 mW per plasma strip).

Example 2: 13.2 W(300 mW per plasma strip).

Optical radiations with these powers can possibly be obtained from semiconductor diode lasers, whose power-generation capability has been increasing in recent years [25].

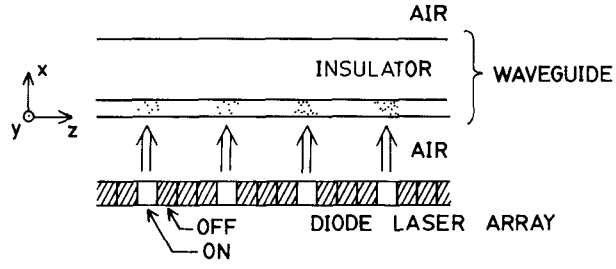

Fig 13. Schematic view of the waveguide illuminated with a semiconductor diode array.

VII. Means of Varying the Period

The period of the light-induced grating in the semiconductor layer can be varied if light sources capable of generating variable illumination patterns are available. A promising light source for such a purpose is a semiconductor diode laser array [19]–[21]. Semiconductor lasers, being very compact, do not spoil the compactness of the grating antenna itself, and have superior electronic controllability.

Let us assume that a diode laser array is placed parallel to the waveguide surface (the semiconductor-film-coated side), as shown in Fig. 13. The emitted lights illuminate the waveguide directly or via transmission lines such as optical fibers. When a two-dimensional array [19], [20] is used, a series of diodes along the y direction is responsible for generating a plasma strip. By turning on the diodes selectively, we can obtain a periodic illumination pattern with a period which is any multiple of the spacing between the individual diodes. Thus the main beam direction can be switched among several directions electronically.

Although the beam steering mentioned above is essentially discrete, almost continuous scanning would be achieved by decreasing the spacing between the emitting elements and increasing the number of diodes.

VIII. Conclusions

We have studied theoretically the radiation characteristics of a periodic dielectric waveguide having a light-induced grating layer. Silicon on sapphire structure has been assumed for the waveguide.

The characteristic equation was derived using a boundary-integral-equation formulation and was solved numerically to give leaky-mode solutions for both TM and TE polarizations. Radiation properties such as the main beam direction, the half-power beam width, and the radiation efficiency are calculated as functions of the electron–hole plasma density and the dimensions of the induced plasma strips. It was shown that narrow beam widths are hard to obtain when operating with TE polarization. Estimations of the illumination power required to realize an antenna were made. Finally, it was mentioned that the waveguide presented in this paper, in conjunction with a high-power semiconductor diode laser array as a light source, may be developed to operate as a leaky-wave antenna at millimeter-wave frequencies whose main beam direction can be switched electronically among several directions.

In the present analysis, we have used a simple model where the plasma distributes itself uniformly in regions with rectangular cross section. In order to predict the radiation properties more precisely, we have to carry out an analysis that includes the effect of the nonuniformity of the plasma distribution arising from carrier diffusion in the direction parallel to the semiconductor film and surface recombination of carriers at the semiconductor–air and semiconductor–insulator interfaces.

References

[1] T. Itoh, "Application of gratings in a dielectric waveguide for leaky-wave antennas and band-reject filters," *IEEE Trans. Microwave Theory Tech.*, vol. MTT-25, pp. 1134–1138, Dec. 1977.

[2] K. L. Klohn, R. E. Horn, H. Jacobs, and E. Freibergs, "Silicon waveguide frequency scanning linear array antenna," *IEEE Trans. Microwave Theory Tech.*, vol. MTT-26, pp. 764–773, Oct. 1978.

[3] F. K. Schwering and S. T. Peng, "Design of dielectric grating antennas for millimeter-wave applications," *IEEE Trans. Microwave Theory Tech.*, vol. MTT-31, pp. 199–209, Feb. 1983.

[4] R. E. Horn, H. Jacobs, E. Freibergs, and K. L. Klohn, "Electronic modulated beam-steerable silicon waveguide array antenna," *IEEE Trans. Microwave Theory Tech.*, vol. MTT-28, pp. 647–653, June 1980.

[5] T. Ohira, M. Tsutsumi, and N. Kumagai, "Radiation of millimeter waves from a grooved ferrite image line," *Proc. IEEE*, vol. 70, pp. 682–683, June 1982.

[6] R. Karg and E. Kreutzer, "Light-controlled semiconductor waveguide antenna," *Electron. Lett.*, vol. 13, pp. 246–247, Apr. 1977.

[7] M. Matsumoto, M. Tsutsumi, and N. Kumagai, "Millimeter-wave radiation characteristics of a periodically plasma-induced semiconductor waveguide," *Electron. Lett.*, vol. 22, pp. 710–711, June 1986.

[8] C. H. Lee, S. Mak, and A. P. DeFonzo, "Millimeter-wave switching by optically generated plasma in silicon," *Electron. Lett.*, vol. 14, pp. 733–734, Nov. 1978.

[9] A. P. DeFonzo, C. H. Lee, and P. S. Mak, "Optically controllable millimeter wave phase shifter," *Appl. Phys. Lett.*, vol. 35, pp. 575–577, Oct. 1979.

[10] C. H. Lee, P. S. Mak, and A. P. DeFonzo, "Optical control of millimeter-wave propagation in dielectric waveguides," *IEEE J. Quantum Electron.*, vol. QE-16, pp. 277–288, Mar. 1980.

[11] K. Ogusu, I. Tanaka, and H. Itoh, "Propagation properties of dielectric waveguides with optically induced plasma layers," *Trans. IECE Japan*, vol. J66-C, pp. 39–46, Jan. 1983.

[12] K. Ogusu and I. Tanaka, "Dielectric waveguide-type millimeter-wave modulator using photoconductivity," *Trans. IECE Japan*, vol. J-67B, pp. 416–423, Apr. 1984.

[13] J. K. Butler, T.-F. Wu, and M. W. Scott, "Nonuniform layer model of a millimeter-wave phase shifter," *IEEE Trans. Microwave Theory Tech.*, vol. MTT-34, pp. 147–155, Jan. 1986.

[14] M. Matsumoto, M. Tsutsumi, and N. Kumagai, "Bragg reflection characteristics of millimeter waves in a periodically plasma-induced semiconductor waveguide," *IEEE Trans. Microwave Theory Tech.*, vol. MTT-34, pp. 406–411, Apr. 1986.

[15] A. M. Vaucher, M. G. Li, and C. H. Lee, "Diode-laser-controlled millimeter-wave propagation in a silicon waveguide," *Electron. Lett.*, vol. 18, pp. 1066–1067, Dec. 1982.

[16] C. H. Lee, A. M. Yurek, M. G. Li, E. A. Chauchard, and R. P. Fischer, "Optoelectronic modulation of millimeter waves in a silicon-on-sapphire waveguide," in *Picosecond Electronics and Optoelectronics*, G. A. Mourou, D. M. Bloom, and C. H. Lee, Eds. New York: Springer-Verlag, 1985, pp. 212–215.

[17] M. Matsumoto, M. Tsutsumi, and N. Kumagai, "Radiation characteristics of a dielectric slab waveguide loaded with thick metal strips," *IEEE Trans. Microwave Theory Tech.*, vol. MTT-35, pp. 89–95, Feb. 1987.

[18] M. Matsumoto, M. Tsutsumi, and N. Kumagai, "Analysis of periodic wavegudies by means of integral equations," The Institute of Electrical Engineers of Japan, Research Rep. EMT-85-63, Oct. 1985.

[19] S. Uchiyama and K. Iga, "Two-dimensional array of GaInAsP/InP surface-emitting lasers," *Electron. Lett.*, vol. 21, pp. 162–164, Feb. 1985.

[20] J. N. Walpole and Z. L. Liau, "Monolithic two-dimensional arrays of high-power GaInAsP/InP surface-emitting diode lasers," *Appl. Phys. Lett.*, vol. 48, pp. 1636–1638, June 1986.

[21] T. H. Windhorn and W. D. Goodhue, "Monolithic GaAs/AlGaAs diode laser/deflector devices for light emission normal to the surface," *Appl. Phys. Lett.*, vol. 48, pp. 1675–1677, June 1986.

[22] E. E. Russell and E. E. Bell, "Optical constants of sapphire in the far infrared," *J. Opt. Soc. Amer.*, vol. 57, pp. 543–544, Apr. 1967.

[23] Y. Marfaing, "Photoconductivity, photoelectric effects," in *Handbook on Semiconductors*, vol. 2. New York: North-Holland, 1980, ch. 7.

[24] S. M. Sze, *Physics of Semiconductor Devices*, 2nd ed. New York: Wiley, 1981, p. 37.

[25] G. L. Harnagel, D. R. Scifres, H. H. Kung, D. F. Welch, P. S. Cross, and R. D. Burnham, "Five watt continuous-wave AlGaAs laser diodes," *Electron. Lett.*, vol. 22, pp. 605–606, May 1986.

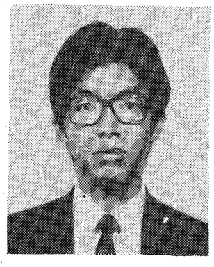

Masayuki Matsumoto (M'85) was born in Osaka, Japan, on January 6, 1960. He received the B.S. and M.S. degrees in engineering from Osaka University, Suita, Osaka, Japan, in 1982 and 1984, respectively.

Since 1985, he has been with the Department of Communication Engineering, Osaka University, where he has been engaged in research on millimeter-wave integrated circuits and components.

Mr. Matsumoto is a member of the Institute of Electronics and Communication Engineers of Japan.

Makoto Tsutsumi (M'71) was born in Tokyo, Japan, on February 25, 1937. He received the B.S. degree in electrical engineering from Ritsumeikan University, Kyoto, Japan, in 1961, and the M.S. and Ph.D. degrees in communication engineering from Osaka University, Osaka, Japan, in 1963 and 1971, respectively.

From 1974 to 1983, he was a Lecturer, and since 1984 he has been an Associate Professor of Communication Engineering at Osaka University. His research interests are primarily in microwave and millimeter-wave ferrite devices. He has published 80 technical papers on these topics in various journals.

Dr. Tsutsumi is a member of the Institute of Electronics and Communication Engineers of Japan and the Japan Society of Applied Physics.

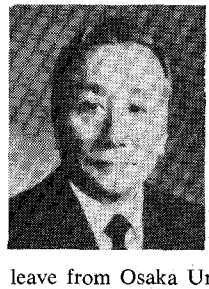

Nobuaki Kumagai (M'59–SM'71–F'81) was born in Japan on May 19, 1929. He received the B. Eng. and D. Eng. degrees from Osaka University, Osaka, Japan, in 1953 and 1959, respectively.

From 1956 to 1960, he was a Research Associate in the Department of Communication Engineering at Osaka University. From 1958 through 1960, he was a Visiting Senior Research Fellow at the Electronics Research Laboratory of the University of California, Berkeley, while on leave from Osaka University. From 1960 to 1970, he was an Associate Professor of Communication Engineering at Osaka University, and

became Professor in 1971. From 1980 to 1982, he served as Dean of Students of Osaka University. In April 1985, he became Dean of Engineering of Osaka University, and he has been President of the university since August of that year. His fields of interest are electromagnetic theory and its applications to microwave, millimeter-wave, and acoustic-wave engineering, optical fibers, integrated optics, and related optical wave techniques, and laser application engineering. He has published more than 100 technical papers on these topics in various journals. He is the author or coauthor of several books, including *Fundamentals of Electromagnetic Theory*, *Microwave Circuits*, and *Introduction to Relativistic Electromagnetic Field Theory*. From 1979 to 1981, he was Chairman of the technical group on Microwave Theory and Techniques of the Institute of Electronics and Communication Engineers of Japan and was Vice President of the Institute of Electronics, Information and Communication Engineers from 1980 to 1982. He is a member of the Telecommunications Technology Council of the Ministry of Post and Telecommunications and the Broadcasting Technology Council of the Japan Broadcasting Corporation (NHK) and is a consultant for the Nippon Telegraph and Telephone Corporation (NTT).

Dr. Kumagai is a member of the Institute of Electronics, Information and Communication Engineers, the Institute of Electrical Engineers of Japan, and the Laser Society of Japan. He has received the Achievement Award from the Institute of Electronics and Communication Engineers of Japan, the Distinguished Services Award from the Institute of Electronics, Information and Communication Engineers, and the Special Achievement Award from the Laser Society of Japan. He was also awarded an IEEE Fellowship for contributions to the study of wave propagation in electromagnetics, optics, and acoustics.